

Collaborative effect of *Csnk1a1* haploinsufficiency and mutant p53 in Myc induction can promote leukemic transformation

Stijn N. R. Fuchs,^{1,2,*} Ursula S. A. Stalman,^{1,2,*} Inge A. M. Snoeren,^{1,2} Eric Bindels,³ Stephani Schmitz,^{1,2} Bella Banjanin,^{1,2} Remco M. Hoogenboezem,³ Stanley van Herk,³ Mohamed Saad,⁴ Wencke Walter,⁵ Torsten Haferlach,⁵ Lancelot Seillier,^{6,7} Julio Saez-Rodriguez,⁹ Aurélien J. F. Dugourd,⁹ Kjong-Van Lehmann,^{6,7} Yinon Ben-Neriah,⁸ Hélène F. E. Gleitz,^{1,2,*} and Rebekka K. Schneider^{1,2,4,*}

¹Department of Developmental Biology, Erasmus Medical Center, Rotterdam, the Netherlands; ²Onco Institute and ³Department of Hematology, Erasmus Medical Center Cancer Institute, Rotterdam, the Netherlands; ⁴Department of Cell and Tumor Biology, Faculty of Medicine, Rheinisch-Westfälische Technische Hochschule Aachen University, Aachen, Germany; ⁵MLL Munich Leukemia Laboratory, Munich, Germany; ⁶Cancer Research Center Cologne Essen, University Hospital Cologne, Cologne, Germany; ⁷Joint Research Center for Computational Biomedicine, University Hospital Rheinisch-Westfälische Technische Hochschule Aachen, Aachen, Germany; ⁸The Lautenberg Center for Immunology and Cancer Research, Institute of Medical Research Israel-Canada, Hebrew University-Hadassah Medical School, Jerusalem, Israel; and ⁹Heidelberg University, Faculty of Medicine, and Heidelberg University Hospital, Institute for Computational Biomedicine, Bioquant, Heidelberg, Germany

Key Points

- *Csnk1a1* haploinsufficiency and p53 mutation collaborate on malignant transformation of hematopoietic stem cells.
- Clonal advantage and leukemic transformation are driven by converging Wnt and Myc signaling.

It is still not fully understood how genetic haploinsufficiency in del(5q) myelodysplastic syndrome (MDS) contributes to malignant transformation of hematopoietic stem cells. We asked how compound haploinsufficiency for *Csnk1a1* and *Egr1* in the common deleted region on chromosome 5 affects hematopoietic stem cells. Additionally, *Trp53* was disrupted as the most frequently mutated gene in del(5q) MDS using CRISPR/Cas9 editing in hematopoietic progenitors of wild-type (WT), *Csnk1a1*^{-/+}, *Egr1*^{-/+}, *Csnk1a1/Egr1*^{-/+} mice. A transplantable acute leukemia only developed in the *Csnk1a1*^{-/+} *Trp53*-edited recipient. Isolated blasts were indefinitely cultured ex vivo and gave rise to leukemia after transplantation, providing a tool to study disease mechanisms or perform drug screenings. In a small-scale drug screening, the collaborative effect of *Csnk1a1* haploinsufficiency and *Trp53* sensitized blasts to the CSNK1 inhibitor A51 relative to WT or *Csnk1a1* haploinsufficient cells. In vivo, A51 treatment significantly reduced blast counts in *Csnk1a1* haploinsufficient/*Trp53* acute leukemias and restored hematopoiesis in the bone marrow. Transcriptomics on blasts and their normal counterparts showed that the derived leukemia was driven by MAPK and Myc upregulation downstream of *Csnk1a1* haploinsufficiency cooperating with a downregulated p53 axis. A collaborative effect of *Csnk1a1* haploinsufficiency and p53 loss on MAPK and Myc upregulation was confirmed on the protein level. Downregulation of Myc protein expression correlated with efficient elimination of blasts in A51 treatment. The “Myc signature” closely resembled the transcriptional profile of patients with del(5q) MDS with *TP53* mutation.

Submitted 12 September 2022; accepted 9 December 2023; prepublished online on *Blood Advances* First Edition 26 December 2023; final version published online 1 February 2024. <https://doi.org/10.1182/bloodadvances.2022008926>.

*S.N.R.F., U.S.A.S., H.F.E.G., and R.K.S. contributed equally to this work.

RNA sequencing data have been deposited in the Zenodo database (doi:10.5281/zenodo.10474240).

All original data are available upon request from the corresponding author, Rebekka K. Schneider (reschneider@ukaachen.de).

The full-text version of this article contains a data supplement.

© 2024 by The American Society of Hematology. Licensed under [Creative Commons Attribution-NonCommercial-NoDerivatives 4.0 International \(CC BY-NC-ND 4.0\)](https://creativecommons.org/licenses/by-nc-nd/4.0/), permitting only noncommercial, nonderivative use with attribution. All other rights reserved.

Introduction

Myelodysplastic syndrome (MDS) is a disease of abnormal blood production that frequently progresses to acute myeloid leukemia (AML). One well defined subgroup of MDS carries a deletion of the long arm of chromosome 5, the most common cytogenetic aberrations in MDS (del(5q) MDS).¹ Although the prognosis of MDS with isolated del(5q) is relatively favorable, aberrations of chromosome 5 are overrepresented in therapy-related myeloid neoplasms (t-MNs) and often occur in combination with *TP53* mutations as well as other cytogenetic abnormalities. T-MNs are associated with an exceedingly poor prognosis with a median survival of 8 months,²⁻⁵ and their treatment is challenging. It is often unsuccessful in extending survival because t-MNs are frequently chemoresistant and prone to relapse even after allogeneic stem cell transplantation.⁶⁻⁸

Extensive research over the last decades has not succeeded in identifying a single tumor suppressor gene in the common deleted region of chromosome 5, and neither have inactivating mutations been found on the remaining allele. This led to the currently prevailing view that the gene dosage of several potentially cooperating candidate genes is responsible in a contiguous gene syndrome.^{4,9} In particular, candidate genes involved in cell cycle regulation, such as *Csnk1a1*, *Egr1*, and *Apc*, have been shown to provide a growth advantage within hematopoietic stem cells (HSCs)¹⁰⁻¹⁶; *Egr1* is a transcription factor involved in multiple cell proliferation pathways. Knockout of *Egr1* in the hematopoietic system leads to increased proliferation and mobilization of HSCs, and *Egr1* haploinsufficiency vastly accelerates the emergence of myeloid and lymphoid malignancies after DNA damage.^{15,16} *Csnk1a1* is a serine/threonine kinase with prominent involvement in Wnt/b-catenin signaling and cell cycle pathways. Our previous work demonstrated that *Csnk1a1* haploinsufficiency leads to a proliferative advantage of HSCs by activation of Wnt signaling and Myc upregulation with concurrent downregulation of inflammatory signaling in HSCs.^{10,17}

TP53 mutations co-occur with chromosome 5 aberrations more frequently than expected by chance, and progression of del(5q) MDS to AML is associated with *TP53* mutation.^{11,18-20} In >90% of the cases, *TP53* mutations in AML involve the DNA-binding domain and are frequently missense mutations.^{5,21} Interestingly, previous studies in mice have found enhanced oncogenic potential of *Trp53* missense mutations compared with *Trp53* loss.²² A dominant negative effect impairing the remaining wild-type (WT) allele has later been demonstrated for the most frequent *TP53* missense mutations of human MDS.²³

It is still unclear how the large heterozygous deletion on chromosome 5 cooperates with *TP53* mutation and/or other genetic aberrations to drive malignant transformation of hematopoietic stem cells. Here, we modeled haploinsufficiency for *Csnk1a1*, *Egr1*, and their compound haploinsufficiency, together with *Trp53* mutation in mice, to explore the potential for malignant transformation.

Methods

Animal studies

Conditional compound haploinsufficiency for *Csnk1a1*, *Egr1*, and *Mx1-Cre* was achieved as described previously.¹⁷ Mouse

experiments were performed according to protocols approved by the Central Animal Committee (Centrale Commissie Dierproeven, The Netherlands; approval number AVD1010020173387).

Bone marrow cells were harvested from a primary transplant of *Csnk1a1^{fl/+} Mx1-Cre⁺* and *Csnk1a1^{fl/+} Egr1^{-/+} Mx1-Cre⁺* and *Egr1^{-/+}* bone marrow cells into wild-type B6.SJL mice. Ckit⁺ cells were isolated and transduced with concentrated lentiviral particles containing the *Trp53* targeting construct or nontargeted guide sequence and SpCas9. Details are supplied in the supplemental Methods.

Trp53 targeting vectors

The lentiviral vectors were based on the pLKO_TRC005 lentiviral backbone.²⁴ Lentiviral particles were produced by transient transfection of 293T cells using Fugene (Promega) and concentrated using ultracentrifugation at 4°C. Details are supplied in the supplemental Methods.

Quantification and statistical analysis

Statistical analysis was conducted using GraphPad Prism version 9.0 or R version 4.0.3. Unless otherwise specified, data are presented as mean ± standard error of the mean. Significance is depicted throughout the manuscript as follows: **P* ≤ .05; ***P* ≤ .01; ****P* ≤ .0001.

Results

Proliferative stem cell phenotype of *Csnk1a1^{fl/+}* and *Csnk1a1^{fl/+}Egr1^{-/+}* mice

We sought to model malignant transformation of hematopoietic stem and progenitor cells (HSPCs) with deletion of key genes on the q-arm of chromosome 5, found to contribute to a growth advantage of hematopoietic stem cells when expressed at haploinsufficient levels.^{10,13,16,17} We transplanted whole bone marrow of *Mx1Cre*, *Csnk1a1^{fl/+}*, *Egr1^{-/+}*, and *Csnk1a1^{fl/+}Egr1^{-/+}* mice (CD45.2⁺) into WT B6 mice (CD45.1⁺), induced excision of the floxed allele after 4 weeks, and tracked the chimerism and blood cell counts over a total of 24 weeks (Figure 1A). All recipients recovered to a donor chimerism (CD45.2⁺) >95% (supplemental Figure 1B). Hemoglobin levels were normal in the recipients' blood over time (supplemental Figure 1A). None of the mice developed spontaneous malignancies during the time of observation (supplemental Figure 1C). The CD11b⁺ myeloid output in the blood of recipients of *Egr1* and *Csnk1a1/Egr1* haploinsufficient bone marrow was increased (Figure 1B). The frequencies of progenitor populations of WT (*Mx1Cre*), *Csnk1a1^{-/+}*, *Egr1^{-/+}*, and *Csnk1a1/Egr1^{-/+}* mice were all comparable and did not show differences (Figure 1C-D).

Colony forming assays demonstrated increased colony formation in *Csnk1a1* haploinsufficient Lin-Sca1+cKit⁺ cells (LSKs) but decreased colony counts for *Egr1*. In a second plating, *Csnk1a1^{-/+}*, *Egr1^{-/+}*, and *Csnk1a1/Egr1^{-/+}* all showed increased colony formation compared with WT (Figure 1E). Bulk RNA sequencing was performed on freshly isolated and sorted LSK hematopoietic progenitors. Transcriptomes of samples clustered together by genotype in principal component analysis (supplemental Figure 1D), and each haploinsufficient genotype was compared with *Mx1Cre* (WT). In general, compound haploinsufficiency for *Csnk1a1* and *Egr1*

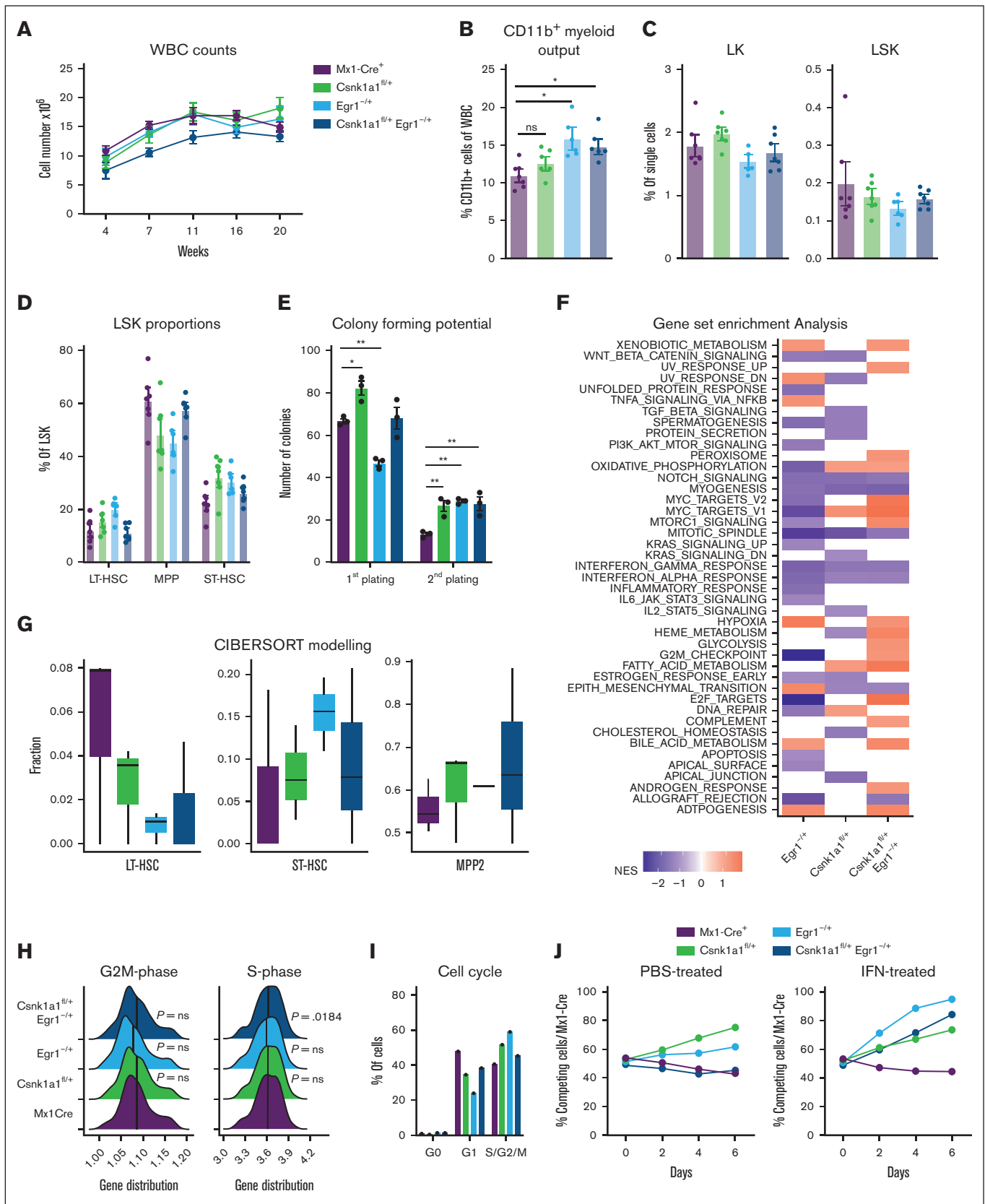


Figure 1. Stem cell phenotype of *Csnk1a1*^{fl/+}, *Egr1*^{-/-} and *Csnk1a1*^{fl/+}*Egr1*^{-/-} mice. (A) White blood cell counts recorded at 4, 7, 11, 16, and 20 weeks after transplant. (B) Frequency of CD11b⁺ myeloid cells of viable blood cells at 20 weeks after transplant (euthanize). (C) Frequency of CD45.2⁺ cells in bone marrow LK (Lin⁻ and kkit⁺) and LSK

caused activation of numerous pathways that were neither activated in *Csnk1a1* nor *Egr1* haploinsufficiency alone. This was particularly pronounced in metabolic pathways such as fatty acid metabolism, glycolysis, mitochondrial iron transport, and complement activation. These factors might contribute to the expansion of hematopoietic cells not only by intrinsic but also extrinsic (environmental) factors. *Csnk1a1* and *Csnk1a1/Egr1* haploinsufficient LSKs further displayed upregulation of proliferation and cell cycle pathways such as *Myc*- and *E2F* targets, whereas these pathways were not upregulated in *Egr1* haploinsufficient LSKs (Figure 1F). Cibersort debulking of the RNA sequencing data demonstrated that the most immature HSC cluster was reduced in the *Csnk1a1*, *Egr1*, and *Csnk1a1/Egr1* condition compared with in the WT sample, whereas the downstream uncommitted progenitors (short-term hematopoietic stem cells [ST-HSC]), intermediate progenitors, such as MPP2) were expanded (Figure 1G). These results were in line with the finding that S-phase-related genes were upregulated in the *Csnk1a1/Egr1* haploinsufficient samples. *Fms*-related tyrosine kinase 3 ligand (FL) estrogen-receptor (ER)-HoxB8 cells were generated as immortalized HSPCs (multipotent progenitor cells) with lymphoid and myeloid differentiation potential (FL-HoxB8 cells). *Csnk1a1* and *Egr1* haploinsufficient cells had a trend of increased cell cycle entry, which was less pronounced for *Csnk1a1^{-/+}/Egr1^{-/+}* (Figure 1H-I). This was also reflected in their competitive advantage (Figure 1J): *Csnk1a1* and *Egr1* haploinsufficient cells outgrew WT competitors over time, whereas *Csnk1a1/Egr1* haploinsufficient cells were more comparable with WT cells as observed in vivo, even under inflammatory stress.¹⁷ Our results, thus, suggest that the transcriptional proliferative signature in *Csnk1a1/Egr1* haploinsufficient clones is not reflected in a functional growth advantage under normal (nonchallenged) conditions. The combination of *Csnk1a1* and *Egr1* haploinsufficiency might provide a proliferative stimulus but is less efficient in preserving and expanding stem cells.

Collaborative effect of *Trp53* mutations with *Csnk1a1* haploinsufficiency

To further test the potential of these haploinsufficient mouse lines for secondary malignant transformation of hematopoietic progenitors, we introduced *Trp53* mutations into *ckit⁺* enriched progenitors (Figure 2A). Mutations were introduced in the DNA-binding domain of the murine *Trp53* gene using CRISPR-Cas9 genome editing in CD45.2⁺ bone marrow progenitors from the murine models with deletion of 1 allele of *Csnk1a1*, *Egr1*, or compound haploinsufficiency before transplant. Gene marking (green, fluorescent protein [GFP]) before transplant varied from 1.7% to 3.7% in cells transduced with either targeted and nontargeted single guide RNA

(sgRNA), comparable with previous reports (supplemental Figure 2A).²⁴ TP53 editing or knockout is known to facilitate spontaneous malignant transformation and has a propensity to cause thymic T-cell lymphomas in mice,^{25,26} a phenomenon that we observed with short latency in all groups subjected to the lentiviral *Trp53*-sgRNA-Cas9 construct transduction but not in the group transplanted with *Mx1-Cre⁺*ntg-sgRNA (Figure 2B; supplemental Figure 2D). Only mice from the *Mx1-Cre⁺* *Trp53* and *Csnk1a1* *Trp53* group developed bone marrow disorders. In these groups, 1 mouse each showed expansion of immature cells in the bone marrow without dissemination in the blood or spleen. Leukemia with blast dissemination and splenomegaly developed in the blood of 1 *Csnk1a1^{-/+}* *Trp53* mouse (Figure 2C-E).

Four weeks after transplantation, blood of mice from all groups had many small *Trp53*-edited clones bearing different indels overall constituting ~5% to 15% of all sequences (Figure 2F; supplemental Figure 2E,F,G), with no specific insertion or deletion size being favored (supplemental Figure 2F). Notably, mouse 00-1, which developed leukemia, had a fraction of small indels overall constituting 15.4% of total sequence traces, comparable with the other experimental mice. The clonal sequence carrying a 13bp deletion was not detected in the blood 4 weeks after the transplant but constituted 80.2% of total sequence traces in the bone marrow at the end of the experiment (Figure 2F).

By flow cytometry, blasts appeared large in forward/side scatter with negativity for lineage markers (Gr1, Ter119, CD11b, CD3, and B220) and positivity for CD48 (Figure 2G), indicative of acute leukemia but ambiguous lineage. Blasts showed a 13 base pair deletion in the DNA-binding domain of the *Trp53* sequence as detected by Sanger sequencing (Figure 2H).

Csnk1a1^{-/+} p53^{mut} leukemia is transplantable and rapidly progressing in secondary recipients

To explore the aggressiveness and transplantability of the generated leukemia, whole bone marrow cells of the initial leukemic mouse (CD45.2) were transplanted into sublethally irradiated CD45.1⁺ secondary recipients (Figure 3A). All recipients showed disease onset ~28 days after transplantation. At this time, blood of all mice showed a CD45.2 chimerism of ~60%, with residual normal hematopoiesis largely derived from 45.1 recipient hematopoiesis (supplemental Figure 4A-B). Three of the 5 recipient mice showed leukocytosis and elevated hemoglobin (Figure 3B). High frequencies of large basophilic blasts were found in the peripheral blood, bone marrow, and spleens of all recipients (Figure 3C-D). Blasts were CD48⁺, CD19-intermediate, CD31-low, Il7ra, CD45.2-low, and negative for *ckit*, Sca1, CD3, Gr1, CD11b, Ter119, B220, CD150, CD115 (m-CSF receptor), CD34,

Figure 1 (continued) (Lin⁻ Sca1⁺ ckit⁺) in bone marrow at 20 weeks after transplant (euthanize). (D) Frequency of MPP (CD48⁺CD150⁻LSK), ST-HSC (CD48-CD150- LSK), and long-term hematopoietic stem cells (CD48-CD150⁺ LSK) in CD45.2⁺ LSK cells in the bone marrow at harvest. (E) Colony forming potential of sorted LSK cells from *Mx1Cre*, *Csnk1a1^{fl/+}*, *Egr1^{-/+}*, and *Csnk1a1^{fl/+}Egr1^{-/+}* mice plated in methylcellulose at first and second plating. (F) Gene set enrichment analysis of Hallmark pathways on RNA sequencing data of sorted LSK; columns signify enriched pathways of contrast *Egr1^{-/+}* vs *Mx1Cre⁺*, *Csnk1a1^{fl/+}* vs *Mx1Cre⁺*, and *Csnk1a1^{fl/+}Egr1^{-/+}* vs *Mx1Cre⁺*. (G) Characterization of cell type proportions of sorted LSK based on Cibersort tumor profiling. (H) Ridgeline plot comparing gene distribution of G2M- and S-phase genes based on Cibersort tumor profiling. (I) Intracellular Ki67 and 7-AAD staining to discriminate the cell cycle phases G0, G1, S-G2-M) within *Mx1Cre*, *Csnk1a1^{fl/+}*, *Egr1^{-/+}* and *Csnk1a1^{fl/+}Egr1^{-/+}* HoxB8-Flt3 cells. (J) Flow cytometric analysis of the competitive coculture assay of HOXB8 cells derived from *Mx1Cre* (GFP⁺) against HOXB8 cells derived from *Csnk1a1^{fl/+}*, *Egr1^{-/+}*, and *Csnk1a1^{fl/+}Egr1^{-/+}* HoxB8-Flt3 cells (GFP⁻) over 6 days. Data represent the mean ± standard error of the mean. Statistical test was performed by 1-way analysis of variance with Dunnet post hoc test to compare each genotype to control (*Mx1Cre*). Only significant results are marked and all other comparisons were nonsignificant. HGB, hemoglobin; IFN, interferon; PBS, phosphate-buffered saline; WBC, white blood cell.

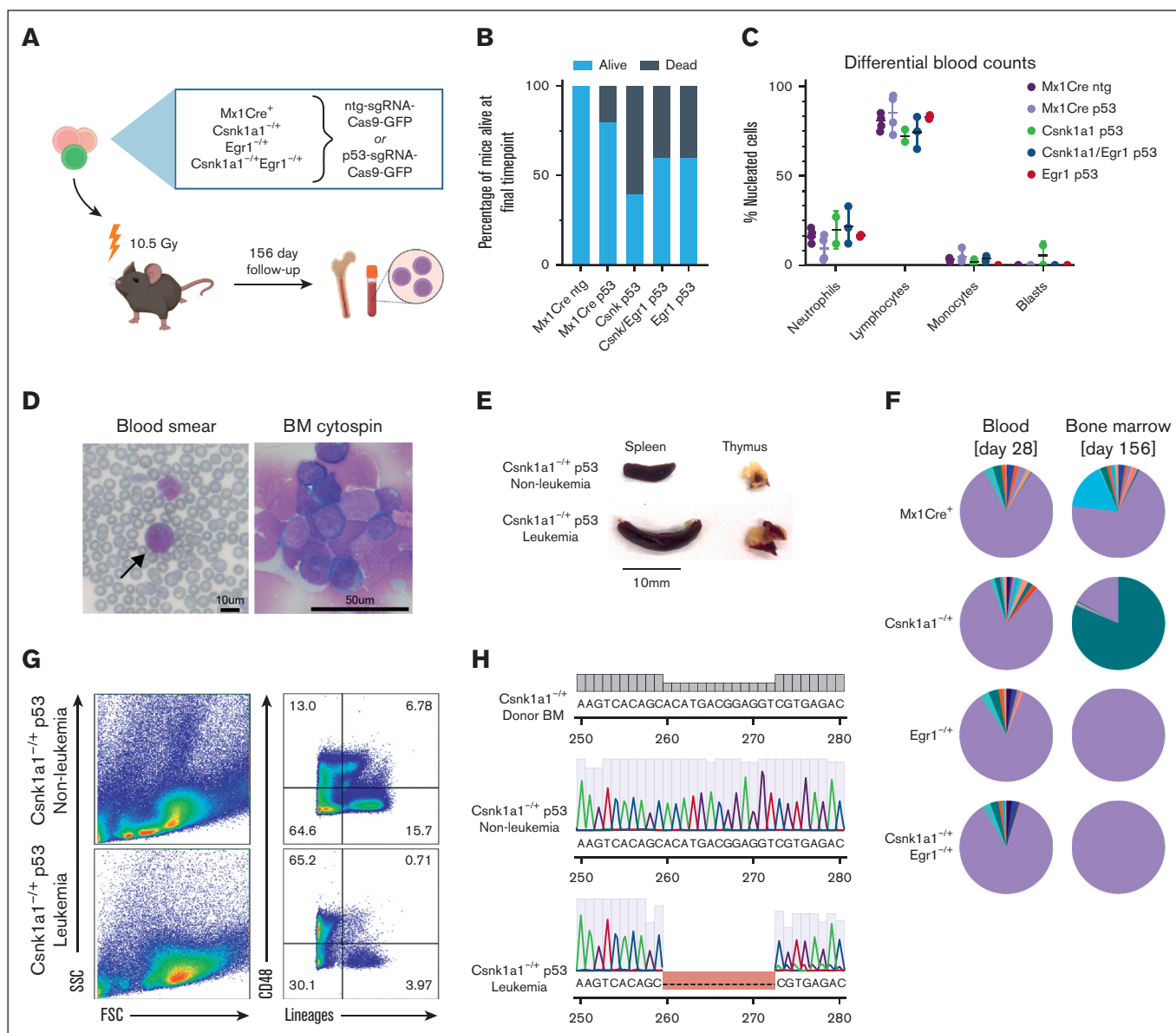


Figure 2. Introduction of *Trp53* mutations into bone marrow progenitors of del(5q) MDS mouse models leads to leukemic transformation in *Csnk1a1*^{-/-} p53^{mut} mouse. (A) Schematic experimental design: WT recipients received transplantation with Mx1-Cre⁺, Csnk1a1^{-/-}, Egr1^{-/-}, and Csnk1a1^{-/-}Egr1^{-/-} bone marrow progenitor cells (ckit⁺) transduced ex vivo with p53-sgRNA⁺Cas9 or ntg-sgRNA⁺Cas9. (B) Frequency of mice alive after 156 days. (C) Differential blood counts in MGG stained blood smears of recipient mice at the time of euthanization (156 days after transplant). (D) MGG staining of peripheral blood smear and bone marrow cytospins of leukemic mouse (00-1). Scale bars, 10 μm in blood smear and 50 μm in bone marrow cytospin. (E) Leukemic mouse 00-1 with peripheral blood blasts exhibited splenomegaly but no thymus tumor. Scale bar denotes 10 mm. (F) Pie charts showing indel distribution among mice with matched samples from peripheral blood, sampled 4 weeks after transplantation (left pie chart), and bone marrow was sampled at harvest (right pie chart). Genomic DNA was extracted, Trp53 amplified, and Sanger sequencing performed. Indel distribution was inferred using Tracking of Indels by Decomposition decomposition of sequence traces. Wild-type Trp53 sequence are in purple, and indels of different bp length are in other colors. (G) Flow cytometry of bone marrow of leukemic mouse (00-1) and nonleukemic control mouse (99-1) shows accumulation of large lineage negative CD48⁺ blasts and depletion of lineage markers expressing differentiated cells. (H) Sanger sequencing of *Trp53* amplicon in leukemic mouse (00-1) bone marrow cells reveals 13bp deletion within DNA-binding domain of Trp53 compared with unedited donor bone marrow sequence (BM before transduction with *Trp53* sgRNA-Cas9 construct) and *Trp53* amplicon of nonleukemic control mouse 99-1. BM, bone marrow.

Thy1.2, NK1.1, and CD135 (Flt3) (Figure 3E), thus indicating a progenitor phenotype but ambiguous lineage. Round-shaped blasts with high nucleus to cytoplasmic ratio were densely packed in hypercellular bone marrows, and also, the spleen showed blast infiltrates (Figure 3F).

We performed exome sequencing on the in vitro cultured blasts and primary and secondary leukemia, comparing leukemic cells with the nontransformed counterparts to exclude additional acquired mutations (Figure 3G). For every gene that contained at least 1 variant, we identified the human-derived homologs. We

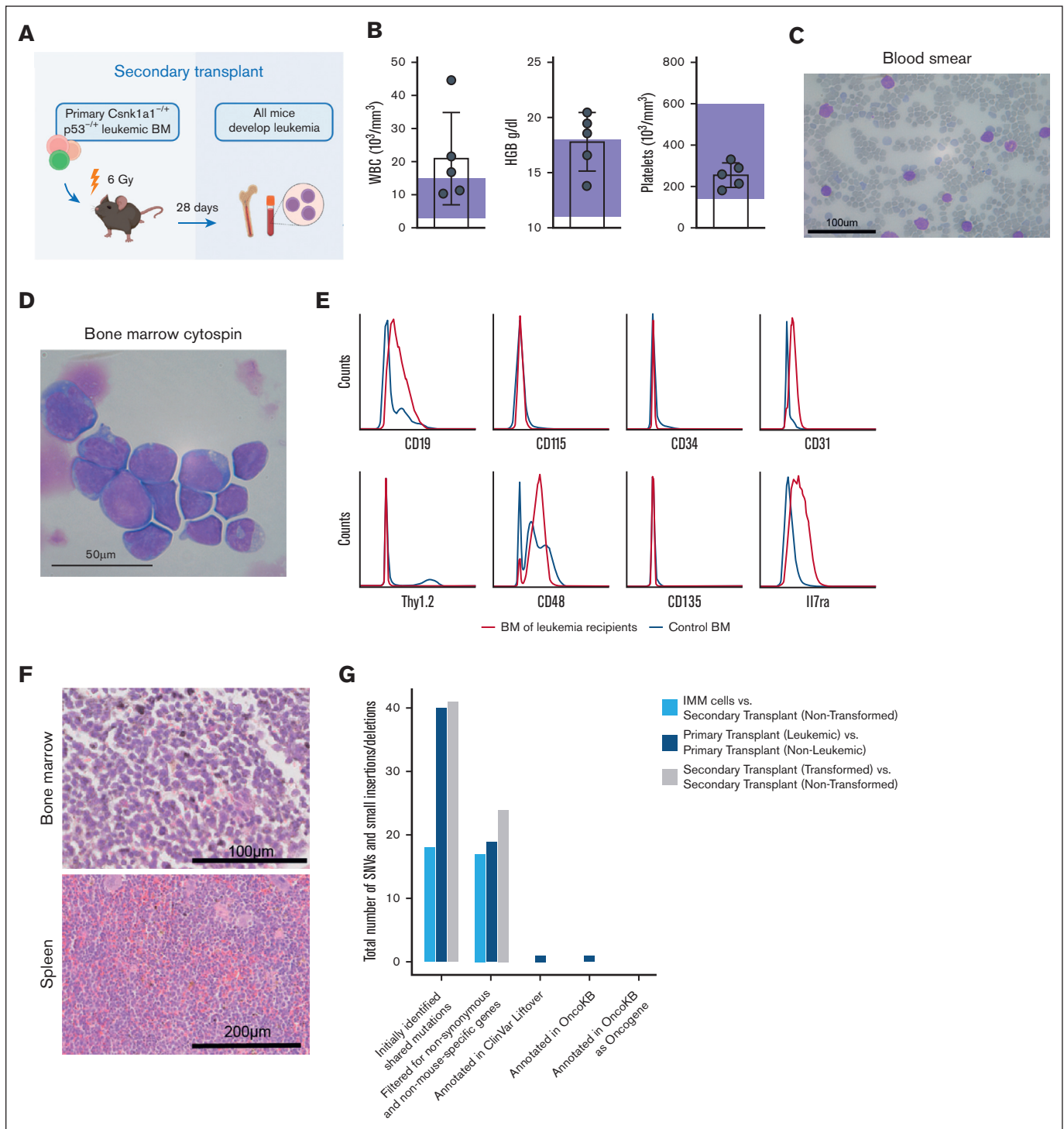


Figure 3. Leukemia is transplantable and rapidly progressing in secondary recipients. (A) Schematic representation of the secondary transplant, in which primary *Csnk1a1*^{-/-}*p53*^{-/-} leukemic bone marrow was transplanted into 5 sublethally irradiated WT recipients and euthanized after 28 days. Secondary recipients of bone marrow cells received sublethal irradiation (6 Gy) and received transplantation with 2.5×10^6 bone marrow cells from leukemic mouse (00-1) each. All mice developed disease rapidly and were moribund within 4 weeks after transplant. (B) Peripheral blood counts at time of euthanasia show leukocytosis and elevated hemoglobin (HGB) levels in 3 of 5 mice. Platelet counts were normal. Reference levels are highlighted by purple rectangles. (C) Peripheral blood smears with MGG staining show infiltration with large basophil blasts. Scale bar, 100 μm . (D) Bone marrow cytopsin with MGG staining show basophil blasts; scale bar, 50 μm . (E) Histograms demonstrating the surface marker expression profile of leukemic blasts analyzed by flow cytometry gated on alive/lineage negative cells. Blue curve represents healthy control bone marrow, and red curve represents bone marrow of leukemic secondary recipients. (F) Hematoxylin and eosin (HE) stainings of femur (scale bar, 100 μm) and spleen (scale bar, 200 μm) sections. (G) Total number of single nucleotide variants and small insertions and deletions identified by whole exome sequencing of immortalized blasts (IMMs), primary transplants (leukemic vs nonleukemic), and secondary transplants (transformed vs nontransformed) after indicated filtering steps.

removed both nonsynonymous and nonhuman mutations. All genes with at least 1 single nucleotide variant remaining were screened for presence in the OncoKB database regarding their cancer gene status. All mutations were annotated using GRCh38 to mm10 liftover of the ClinVar annotation database for their predicted clinical significance. Mutations were manually rechecked in the University of California, Santa Cruz genome browser for correct mapping of the liftover positions found in the ClinVar annotation database. Genes were not considered further if neither was being marked as oncogene in OncoKB nor being "likely pathogenic" nor of "unclear significance" in the ClinVar Liftover database. After these careful filtering steps, only the primary transplant leukemia had 1 overlap with OncoKB genes affecting the gene *Taf4*. We next interrogated a cohort of samples from patients with *del(5q)* MDS for this mutation. None of the 98 patients with *del(5q)* MDS (with or without TP53 mutation) had a TAF4 mutation. Additionally, we looked at the expression level of TAF4 in the different World Health Organization MDS diagnosis groups (total of 669 patients). We did not detect any significant differences among the different groups in TAF4 expression. Because this variant was also not identified in the secondary transplant, we concluded that it is likely not a driver of the disease.

Leukemic blasts can be cultured ex vivo and are susceptible to direct *Csnk1a1* and *Cdk7/9* inhibition

We next asked whether primary blasts were expandable ex vivo in a liquid culture system (Figure 4A). Blasts did not grow in methylcellulose or conventional stem cell medium (CellGro media supplemented by murine stem cell factor and murine thrombopoietin; data not included). Primary leukemic blasts were propagated on OP9 feeder cells in cell culture medium supplemented with Flt-3 and Il7, on which they started expanding after 3 weeks of culturing and weekly transferal onto fresh feeder cells. Cultured blasts reflect the phenotype in vivo characterized by large indented nuclei surrounded by basophilic cytoplasm and often atypical mitotic figures (Figure 4B). We confirmed that the ex vivo cultured blasts were the cells carrying the previously found 13bp deletion in the *Trp53* allele and that they retained morphology and immunophenotype of the primary blasts (*Lin*⁻, *CD45.2*⁺, *Il7ra*⁺, *CD48*⁺, *CD19*^{low}, and *CD31*^{low}).

A leukemia cell line that can be modified in vitro and then studied in vivo would be a good tool to understand, for example, druggable pathways in the context of *Csnk1a1* haploinsufficiency as a relevant gene in the HSC phenotype and targeted therapy of *del(5q)* MDS.¹⁰ We, thus, transplanted cultured blasts into sublethally irradiated mice and compared them with transplanted secondary leukemia transplants as controls. At 4 weeks, mice developed signs of disease in similar kinetics to the transplanted secondary leukemia (Figure 4C). In 2 of 3 mice, the blast counts in the blood and bone marrow were comparable with that of control leukemias and nearly encompassed 100% of bone marrow cells, which was reflected in a hypercellular bone marrow (Figure 4D-E). Morphologically, the bone marrow was filled with small blasts with high nucleus-cytoplasm ratio, with complete replacement of trilineage hematopoiesis in the bone marrow and, thus, in line with the original leukemia phenotype (Figure 4F).

Having generated these expandable and transplantable blasts, we performed a small-scale, proof-of-concept drug screening informed

by previous studies. We compared the *Csnk1a1/Trp53* blasts with *Hoxb8* overexpressing cells derived from *Csnk1a1*^{-/+} *Mx1Cre*⁺ and *Mx1Cre*⁺ mice with intact p53 (hereafter referred to as *Csnk1a1*^{-/+} *Hoxb8*-Flt3 and WT *Hoxb8*-Flt3 cells). Nutlin-3a inhibits binding of *MDM2* to p53, thereby preventing p53 degradation and activating p53-dependent apoptosis (Figure 4G). In vitro expanded blasts were not sensitive to Nutlin-3a treatment, whereas *Csnk1a1*^{-/+} *Hoxb8*-Flt3 and WT *Hoxb8*-Flt3 cells showed dose-dependent growth arrest. This confirms an impaired function of p53 mutant protein in leukemic blasts. Previous experimental results have demonstrated that *Csnk1a1* haploinsufficient cells are sensitive to *Csnk1a1* knockdown but not in the context of p53 loss.^{10,11} We tested the sensitivity of in vitro expanded blasts to direct *Csnk1a1* inhibition (D4476, A51) and Aurora kinase inhibition, which inhibits growth and survival of AML cell lines in preclinical studies.²⁷ Interestingly, *Trp53* mutant blasts were insensitive to Aurora A kinase inhibition with Alisertib. Direct *Csnk1a1* inhibition using D4476 was not significantly more efficient in *Csnk1a1*^{-/+} *Hoxb8*-Flt3 cells and blasts than in WT *Hoxb8*-Flt3 cells. However, direct *Csnk1a1* and *Cdk7/9* inhibition with compound A51 notably caused growth arrest selectively in *Trp53* mutant blasts at higher dose (Figure 4G).

A51 cotargeting *CKIα* and *CDK7/9* can eradicate blasts in tertiary leukemias

Because A51 selectively targeted *Trp53* mutant blasts in the proof-of-concept drug screening, we next set out to validate this finding in a tertiary leukemia (after sublethal irradiation) in vivo (Figure 5A). Oral treatment was initiated at 8 days after leukemia cell inoculation. Mice in the vehicle group demonstrated leukocytosis and thrombocytopenia ~4 weeks after leukemia inoculation. Blood counts were normalized upon treatment with A51 (Figure 5B), and in particular, the spleen size was reduced (Figure 5C), whereas vehicle-treated mice showed leukemic cell infiltration into the peripheral blood, and blasts were reduced or even absent in 7 of 10 A51-treated mice (Figure 5D). Blasts in the bone marrow were reduced (even if not significant) in A51-treated leukemias, and importantly, the cellularity of the bone marrow was significantly lower (normocellular) than hypercellular bone marrow with dense blasts in the vehicle-treated group (Figure 5D-E). In the A51-treated group, the bone marrows were normocellular, and blasts were loosely scattered, indicating a positive effect of A51 in eliminating blasts and restoring the bone marrow composition.

Leukemic growth is driven by Wnt and *Myc* signaling

To investigate the molecular pathways responsible for driving blast growth, we sorted primary blasts from the initial leukemic mouse and secondary recipients for RNA sequencing (supplemental Figure 6A). As controls, we sorted the corresponding cell population from a healthy *Csnk1a1*^{-/+} *Trp53*-mutated littermate as well as *Mx1Cre*⁺-*Trp53* *mut* and *Mx1Cre*-ntg mice (supplemental Figure 6A). In principal component analysis of transcriptome data, all leukemia samples clustered together, indicating similarity in overall gene expression between primary and secondary leukemias, whereas all controls were clearly separated from the leukemic samples (supplemental Figure 6E). Because the blasts phenotypically characterized as *CD48*⁺, *CD19* intermediate, *CD31* low, *Il7ra*, *CD45.2* low and negative for *ckit*, *Sca1*, *CD3*, *Gr1*, *CD11b*, *Ter119*, *B220*, *CD150*, *CD115* (m-CSF receptor), *CD34*,

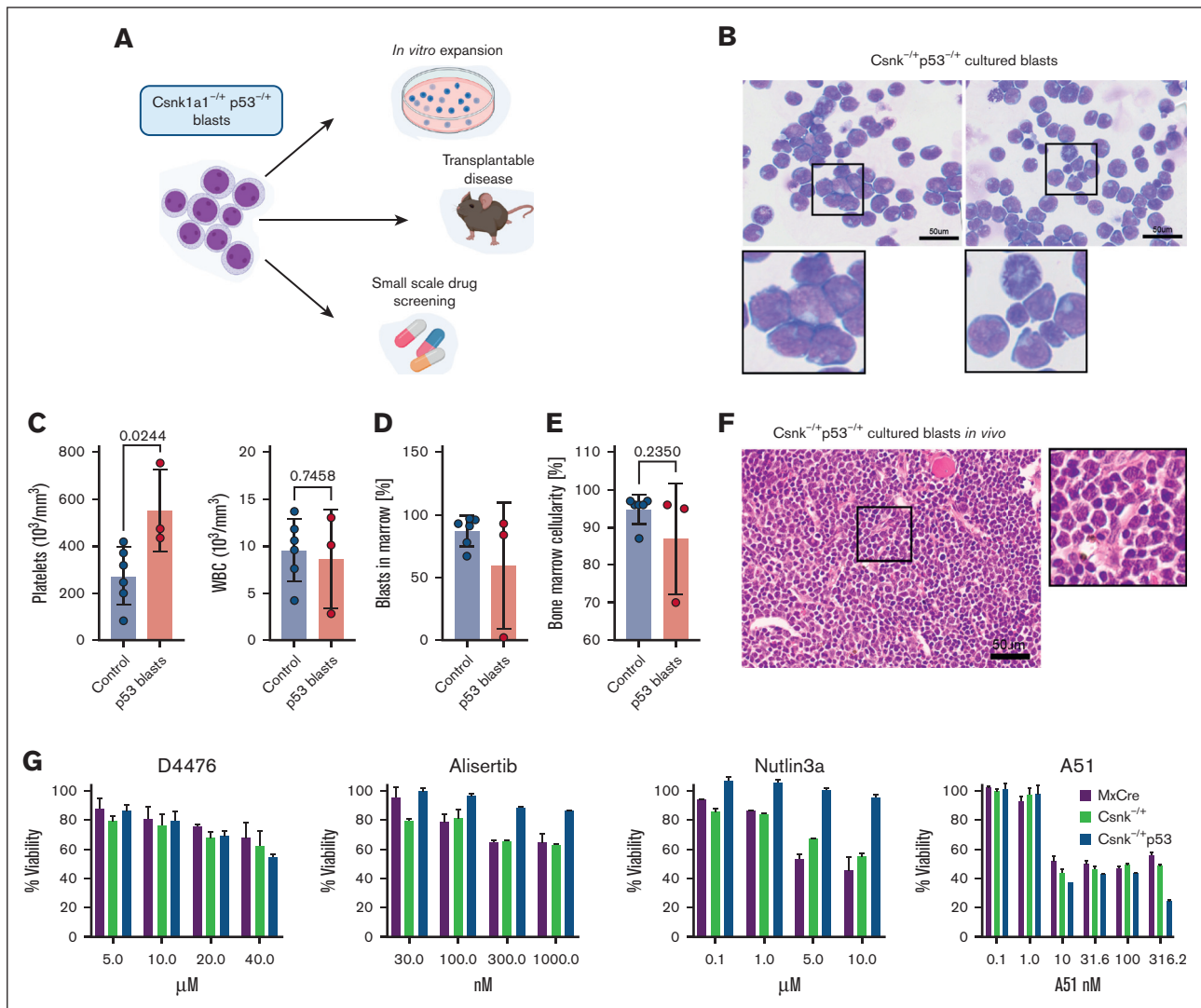


Figure 4. Leukemic blasts can be cultured ex vivo and retransplanted and are susceptible to direct *Csnk1a1* and CDK7/9 inhibition. (A) Scheme showing the potential applications of leukemic blasts: *Csnk1a1*^{-/-}*p53*^{-/-} were expanded in vitro, transplanted into sublethally irradiated recipients, and used for small-scale drug screening based on viability. (B) In vitro expanded *Csnk1a1*^{-/-}*p53*^{mut} blasts retain morphology of initial disease. Scale bar, 50 μm . (C) Platelet and white blood cell counts of sublethally irradiated (6 Gy) WT recipients of leukemic *p53* blasts expanded in vitro ($n = 3$ mice) compared with controls with transplanted secondary leukemias. (D) Blast cells in the bone marrow were detected in 2 out of 3 mice that received transplantation with leukemic *p53* blasts and compared to secondary leukemia transplants. (E) Bone marrow cellularity in mice that received transplantation with leukemic *p53* blasts expanded in vitro. (F) HE staining of bone marrow (femur) section of mice transplanted with leukemic *p53* blasts expanded in vitro. (G) Cell proliferation and survival (percentage viability) measured by MTT assay of cultured blasts (*Csnk1a1*^{-/-}*p53*), *Csnk1a1*^{-/-} Hoxb8-Flt3, and WT Hoxb8-Flt3 cells subjected to increasing doses of D4476, A51, Alisertib, and Nutlin3a.

Thy1.2, NK1.1, and CD135 (Flt3), indicating a progenitor phenotype but ambiguous lineage, we first asked how they compared with normal HSPCs^{17,28} and previously characterized murine leukemias using CIBERSORT.^{17,29} Sort-purified blasts had transcriptional similarity with MPP2 as a myeloid biased progenitor with multilineage potential but not ST- and long-term hematopoietic stem cells (Figure 6A). When compared with different types of acute leukemia, the sort-purified blasts had high transcriptional similarity to acute erythroid leukemia, some similarity to AML but, interestingly, not to lymphoblastic leukemia (Figure 6B). Based on the indicated erythroblastic transcriptional signature (supplemental Figure 6D), we analyzed Ter119/CD71 expression commonly

used in the characterization of murine erythroid cells. In line with the progenitor status, the blasts were characterized by high expression of CD71 but negativity for Ter119 (supplemental Figure 6B). High expression of CD71 in the literature is associated with poor survival, poor differentiation, and is a marker of proliferation in both lymphoid and myeloid neoplasms. Based on these results and also recommendations of the recent World Health Organization classification and reviewed in Weinberg and Arber, we conclude that the generated leukemia is an acute leukemia of ambiguous lineage because the leukemia shows evidence for myelo(erythroid) and partially B-lineage commitment, which is characterized by clonal proliferation of primitive hematopoietic

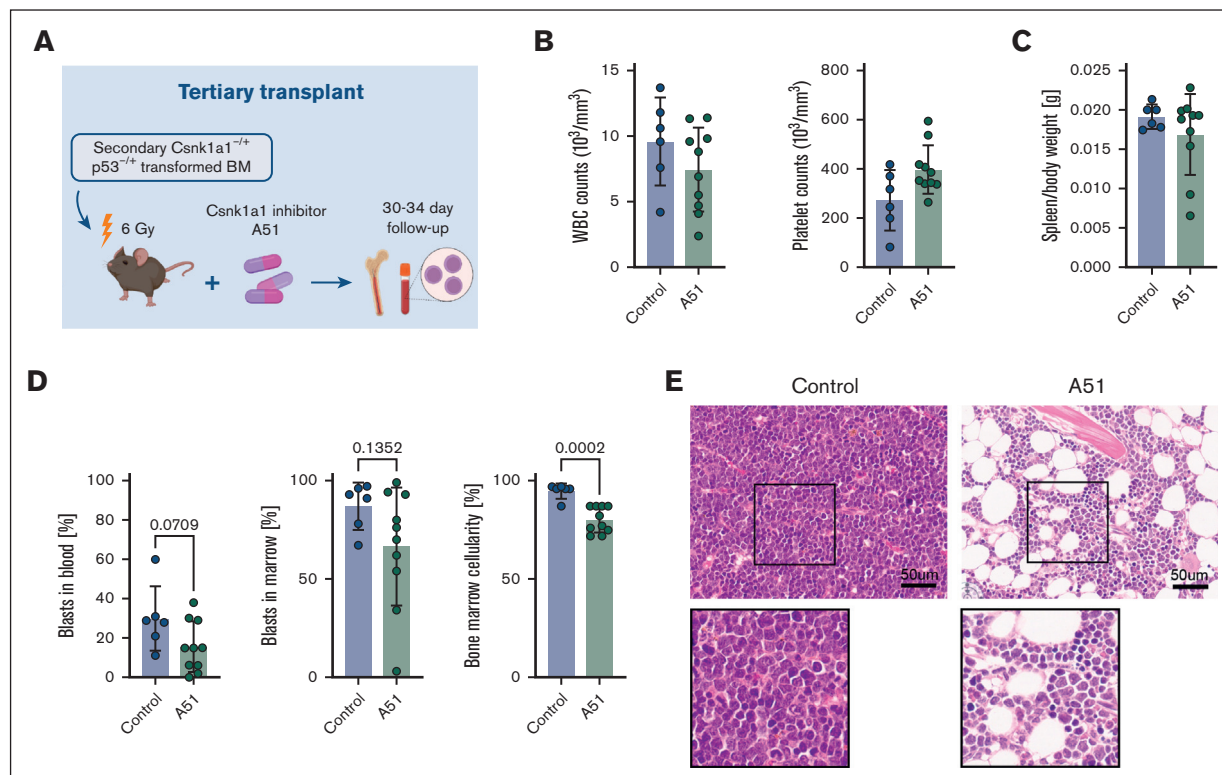


Figure 5. *Csnk1a1*^{-/-}Trp53 mutant leukemias in tertiary transplants are sensitive to A51 treatment. (A) Schematic representation of tertiary sublethally irradiated (6 Gy) WT recipients of secondary *Csnk1a1*^{-/-}p53^{-/-} transformed bone marrow cells (untreated controls, n = 6; A51-treated, n = 10). A51-treated mice received A51 compound (5 mg/kg per day) starting at 8 days after transplant, 5 days per week until 4 weeks after transplant (euthanasia). (B) White blood cell and platelet counts of control and A51-treated mice at 4 weeks after transplant (euthanasia). (C) Spleen-to-bodyweight ratio in control and A51-treated mice. (D) Percentage of blasts in peripheral blood and bone marrow, and bone marrow cellularity in control and A51-treated mice at 4 weeks after transplant (euthanasia). (E) HE staining of bone marrow (femur) sections (scale bar, 50 μ m).

progenitor cells.³⁰ The immature, progenitor status is further evidenced by upregulation of markers summarized as immature myeloid progenitors (supplemental Figure 6C). Pathway footprint analysis predicted downregulation of p53 pathways, as expected, and NF- κ b and hypoxia pathways, whereas MAPK and Wnt signaling were upregulated (Figure 6C-D), as also seen in *Csnk1a1* haploinsufficient hematopoietic stem cells (compare Figure 1).¹⁷ NF- κ b and tumor necrosis factor α signaling were downregulated compared with *Csnk1a1* haploinsufficient HSPCs, clearly reflecting the *Csnk1a1* haploinsufficiency background even in the context of p53 dysfunction.

Bcl2 was the most significantly downregulated gene in leukemia compared with the control samples (Figure 5E). *Bcl2* expression has been demonstrated to be controlled by p53 expression, with mutant p53 overexpression reportedly resulting in *Bcl2* downregulation.³¹ Transcription factor target expression enrichment analysis suggested upregulation of *Myc* and *E2f* activity (Figure 6C), likely contributing to malignant growth in these cells. Accordingly, we found *Myc* targets to be overexpressed in leukemic blasts, specifically peroxiredoxin 4 (*Prdx4*) (Figure 6F).

Network contextualization with prior knowledge interactomes was applied using the bioinformatic tool CARNIVAL³² to make a prediction about the collaborating effect of *Csnk1a1* haploinsufficiency and p53 dysfunction in leukemic blasts. Predictions suggest that *Csnk1a1* haploinsufficiency led to upregulation of the

Wnt-pathway, via upregulation of GSK3B and through *Lrp6*, ultimately culminating in *Lef1* upregulation, known for its role in malignant hematopoietic disorders.³³ *Csnk1a1* haploinsufficiency and p53 downregulation converged on MAPK signaling (as the top upregulated pathway; compare Figure 6D) and NF- κ B/interferon response factors downregulation (*Rela*, *Stat1*, *Stat2*, and *Irf1*). Ultimately, Wnt signaling activated by *Csnk1a1* haploinsufficiency, NF- κ B downregulated by p53 inhibition, and MAPK signaling activated by both alterations finally culminated in activation of the proto-oncogene *Myc* (Figure 6G).

Because MAPK was the top upregulated pathway in the pathway analysis and MAPK1 (ERK2), MAPK3 (ERK1), and MAPK8 (JNK1/2) form a central hub (triangle) in the converging mechanism of *Csnk1a1* haploinsufficiency and Trp53 mutation, we validated their expression on the protein level (Figure 6H). *Csnk1a1* haploinsufficiency increased the expression of JNK1/2 and ERK1/2 compared with WT controls, and the effect was enhanced in the presence of mutant Trp53. *Myc* induction was only observed in the *Csnk1a1/Trp53* mutant blasts but not in *Csnk1a1* haploinsufficiency or WT cells alone, indicating that *Myc* induction is leukemia specific. We were, thus, then wondering whether A51 treatment affects *Myc* expression at the protein level. Interestingly, vehicle-treated leukemias showed a strong induction of *Myc*, whereas A51 treatment significantly reduced the expression (Figure 6I). Notably, good responders to A51 (as indicated by bone

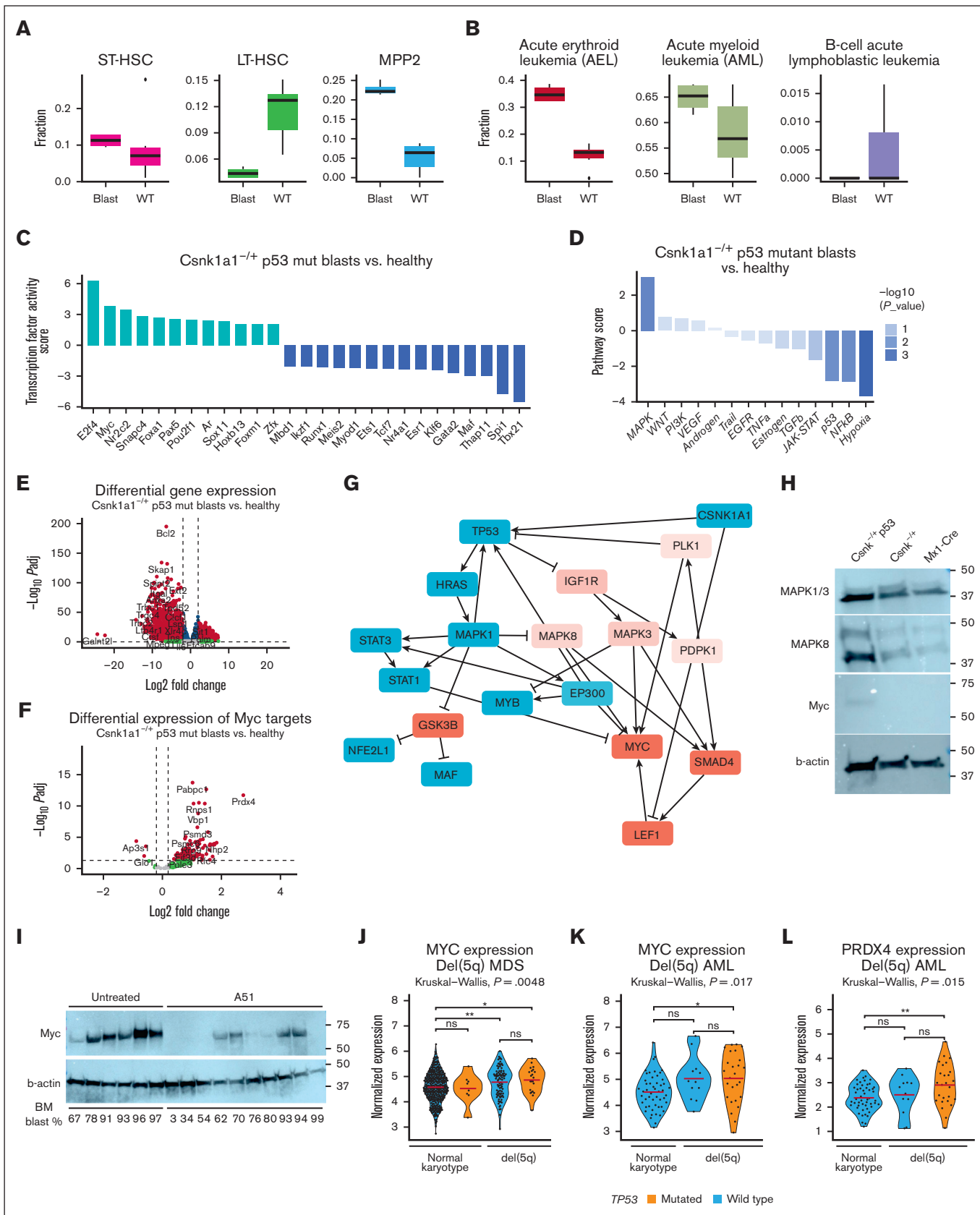


Figure 6.

marrow blast frequency) showed lower expression of *Myc*, indicating that targeting *Myc* is an interesting therapeutic avenue in TP53 mutant disease.

To determine whether MYC expression is also relevant in human del(5q) MDS and human AML with p53 mutation, we analyzed RNA sequencing data of whole bone marrow from patients with del(5q) with and without *TP53* mutation and compared *MYC* expression levels with those of patients with MDS with normal karyotype with and without *TP53* mutation (Figure 6). We observed significant upregulation of *MYC* expression in del(5q) samples from patients (Figure 6J). Furthermore, we tested the expression of *MYC* and top upregulated *MYC* targets in our murine leukemia and in samples from patients with AML with del(5q) or normal karyotype (Figure 6K). Interestingly, *MYC* and also the peroxiredoxin 4 (PRDX4) were significantly upregulated in samples from patients with AML with del(5q) and p53 mutation (Figure 6K-L), reflecting the findings in *Csnk1a1* haploinsufficiency leukemia model.

Discussion

TP53 mutations occur in lower-risk del(5q) MDS at a frequency of ~20% and are associated with a poor prognosis. Progression of del(5q) MDS into secondary acute leukemia has been reported to be linked to clonal evolution of *TP53*-mutated subclones.³⁴ We observed leukemic transformation of murine *Csnk1a1* haploinsufficient HSCs with *Trp53* mutation, recapitulating a genetic murine model of secondary/therapy-related AML with del(5q) and *Trp53* mutation. This disease is transplantable and can be indefinitely cultured ex vivo. We constructed a putative signaling network by comparing the transcriptome of blasts with that of their healthy counterparts that converged on upregulated MAPK signaling (MAPK1/3/8), which we confirmed to be upregulated in *Csnk1a1* haploinsufficiency but even enhanced in *Csnk1a1 Trp53*-mutant leukemia. Activated MAPK, WNT, and NF- κ B signaling were further predicted to culminate in MYC activation. We confirmed that MYC expression is specific for the *Csnk1a1/Trp53* leukemia at the protein level.

As a proof of concept that the derived leukemia can be a useful tool to identify (druggable) mechanisms in leukemia in the context of *Csnk1a1* haploinsufficiency, we performed a small-scale small-molecule inhibitor test. Targeting *Csnk1a1* and the transcriptional

kinases CDK7/9 using compound A51 can be effective at inhibiting growth of *Csnk1a1/Trp53* mutated blasts in vitro and in vivo. A51 treatment reduced *Myc* expression in the bone marrow, and “nonresponders” had higher *Myc* expression, suggesting that *Myc* is an attractive target in more aggressive TP53-mutant disease. *MYC* is also upregulated in MDS and in AML with del(5q) compared with MDS and AML with normal karyotype with and without p53 mutation, supporting the rationale for targeting MYC. In a recent murine model of malignant transformation of clonal hematopoiesis with *Tet2* mutation, depletion of *Traf6* led to myeloid malignancies driven by *Myc* activation.³⁵ Furthermore, t-AMLs with del(5q) show a distinct transcriptomic signature, different from t-AML with other genetic background. They are characterized by the upregulation of genes involved in cellular proliferation including cell cycle control genes and most notably upregulation of *MYC* oncogene and Wnt-signaling upregulation.^{36,37}

The leukemic transformation occurred in the *Csnk1a1* haploinsufficient background and not in the context of *Csnk1a1/Egr1* compound haploinsufficiency.^{9,17} We did not observe a higher rate of malignant hematopoietic transformation (thymic T-cell lymphoma etc) in *Egr1*^{-/+} *Trp53*-mutant or *Csnk1a1*^{-/+} *Egr1*^{-/+} *Trp53*-mutant mice. We observed previously that *Egr1* haploinsufficient HSCs have the potential to clonally expand but show large variability among recipients.¹⁷ Here, we investigated the transcriptome of *Egr1*^{-/+} LSK, which showed deregulation of metabolic pathways but overall downregulation of cell cycle and proliferation related pathways. Stoddart et al elegantly demonstrated how haploinsufficiency for both *Egr1* and *Apc* together with p53 loss creates an environment that is permissive to malignant transformation of HSCs. AML spontaneously occurred in these mice with a long latency of 234 to 299 days.³⁸ The addition of alkylating-agent exposure to the bone marrow niche of both donor and recipient resulted in the emergence of myeloid neoplasm from *Egr1*^{-/+} *Apc*^{-/+} *Trp53*-knockdown HSCs with higher incidence and shorter latency (200 days).³⁹ In line with our findings, this suggests that the true potential for clonal expansion and, therefore, malignant transformation of *Egr1* is highly dependent on the individual microenvironmental context, possibly by metabolic regulation within the surrounding niche. Recent findings additionally suggest that *EGR1* is not strictly haploinsufficient in patients with del(5q) MDS, and *EGR1* expression is not correlated with allele burden.⁴⁰

Figure 6. Leukemic growth is driven by MAPK signaling and Myc activation. (A) Transcriptional blast identified based on Cibersort profiling using published single cell data sets, specifically focusing on short-term and long-term stem cells, and multipotent progenitors. (B) Characterization of disease similarity of p53 blasts based on Cibersort profiling, published RNA sequencing data sets of murine leukemias with focus on acute erythroid leukemia (AEL), AML, and B-cell acute lymphoblastic leukemia (B-ALL). (C) Estimating the activity of transcription factors based on abundance changes of their targets (input: full list of differentially expressed gene blasts vs control) as a proxy of their activity using method DoRothEA positive scores to determine transcription factor (TF) in blasts compared with the nonleukemic controls. (D) Pathway response signature scores for 14 pathways inferred from differentially expressed genes between *Csnk1a1*^{-/+} p53mut leukemic blasts vs nonleukemic control using the method PROGENy (pathway responsive genes for activity inference). (E) Volcano plot showing differentially expressed genes between leukemic blasts vs control. Positive Log2FC: overexpressed in blasts; negative Log2FC: downregulated in blasts. (F) Volcano plot showing differentially expressed genes between *Csnk1a1*^{-/+} p53mut leukemic blasts vs control with genes belonging to Hallmark pathway “MYC targets.” Positive Log2FC: overexpressed in blasts; negative Log2FC: downregulated in blasts. (G) Putative interactome downstream of p53 dysfunction and *Csnk1a1* haploinsufficiency inferred using method CARNIVAL (CAusal Reasoning for Network identification using Integer VALue programming). (H) Western blot analysis of MAPK1/3, MAPK8, *Myc*, and b-actin in *Csnk*^{-/+} p53 blasts, *Csnk1a1*^{fl/+} or Mx1-Cre HoxB8-Fit3 cells. (I) Western blot analysis of *Myc* and B-actin on bone marrow samples of mice that underwent tertiary transplantation and were untreated or treated with A51 compound (related to Figure 5). Blast percentage found in bone marrow is depicted at the bottom of the blot. (J) MYC expression in RNA sequencing data of 114 samples from patients with del(5q) MDS (p53 mutation, n = 22; p53 WT, n = 92) and 400 samples of MDS with normal karyotype (p53 mutation, n = 8; p53 WT, n = 392). (K) MYC expression in RNA sequencing data of 38 samples from patients with AML with del(5q) (p53 mutation, n = 26; p53 WT, n = 12) and 51 samples from patients with AML with normal karyotype and wild-type p53. (L) PRDX4 expression in RNA sequencing data of 38 samples from patients with AML with del(5q) (p53 mutation, n = 26; p53 WT, n = 12) and 51 samples from patients with AML with normal karyotype and wild-type p53.

Combination of *Csnk1a1* and *Egr1* haploinsufficiency provides a proproliferative stimulus to committed progenitors but is less efficient in preserving and expanding stem cells, in line with our previous findings on the role of these 2 genes in the clonal expansion.¹⁷ In comparison, *Csnk1a1* haploinsufficiency drives a robust pro-proliferative phenotype that is enhanced under environmental stress providing selective pressure.¹⁷ As we and others have shown, the pro-proliferative phenotype is dependent on Wnt-signaling dosage.^{10,17,37} This pro-proliferative drive predisposes HSCs to malignant transformation, which is guarded by p53 unless it loses its function in a second-hit event.

Previous work on creating murine models for malignant transformation of del(5q) MDS have used complete *Trp53* loss or *Trp53* knockdown by shRNA.^{38,39} It is still a topic of discussion whether missense P53 mutants have the same function regardless of mutation site or whether they each represent a unique oncogene ranging from loss-of-function, gain-of-function, or dominant negative effect, depending on the cellular context.⁴¹ For human AML, a dominant negative effect of several common heterozygous missense p53 mutations on the WT allele has been demonstrated.²³ In our study, using CRISPR/Cas9 genome editing, we introduced monoallelic and biallelic insertions and deletions in the DNA-binding domain of *Trp53* in a small subset of the HSC pool. Therefore, only cells with advantageous mutations would outgrow WT HSCs. This resembles the situation of patients with clonal selection of hematopoietic progenitors with somatic *TP53* mutations.

Acknowledgments

R.K.S. is an Oncode Institute investigator.

This work was supported by a KWF Kankerbestrijding Young Investigator grant (11031/2017–1, Bas Mulder Award, Dutch Cancer Foundation), grants of the German Research Foundation (CRU344-4288578857858; CRU344-17911533), a grant from the European Research Council (deFIBER; ERC-StG 757339),

References

1. Haase D, Germing U, Schanz J, et al. New insights into the prognostic impact of the karyotype in MDS and correlation with subtypes: evidence from a core dataset of 2124 patients. *Blood*. 2007;110(13):4385-4395.
2. Christiansen DH, Andersen MK, Pedersen-Bjergaard J. Mutations with loss of heterozygosity of p53 are common in therapy-related myelodysplasia and acute myeloid leukemia after exposure to alkylating agents and significantly associated with deletion or loss of 5q, a complex karyotype, and a poor prognosis. *J Clin Oncol*. 2001;19(5):1405-1413.
3. Lindsley RC, Mar BG, Mazzola E, et al. Acute myeloid leukemia ontogeny is defined by distinct somatic mutations. *Blood*. 2015;125(9):1367-1376.
4. McNerney ME, Godley LA, Le Beau MM. Therapy-related myeloid neoplasms: when genetics and environment collide. *Nat Rev Cancer*. 2017;17(9):513-527.
5. Rucker FG, Schlenk RF, Bullinger L, et al. TP53 alterations in acute myeloid leukemia with complex karyotype correlate with specific copy number alterations, monosomal karyotype, and dismal outcome. *Blood*. 2012;119(9):2114-2121.
6. Yoshizato T, Nannya Y, Atsuta Y, et al. Genetic abnormalities in myelodysplasia and secondary acute myeloid leukemia: impact on outcome of stem cell transplantation. *Blood*. 2017;129(17):2347-2358.
7. Lindsley RC, Saber W, Mar BG, et al. Prognostic mutations in myelodysplastic syndrome after stem-cell transplantation. *N Engl J Med*. 2017;376(6):536-547.
8. Garderet L, Ziagkos D, van Biezen A, et al. Allogeneic stem cell transplantation for myelodysplastic syndrome patients with a 5q deletion. *Biol Blood Marrow Transplant*. 2018;24(3):507-513.
9. Ebert BL. Molecular dissection of the 5q deletion in myelodysplastic syndrome. *Semin Oncol*. 2011;38(5):621-626.

and a ZonMW VIDI 09150172110021 (R.K.S.). U.S.A.S. was supported by a research fellowship by the IMF University of Münster (ST521701) and by a research fellowship from the German Research Foundation (STA 1648/1-1). This work was further supported by a grant of the José Carreras Leukemia Foundation (R.K.S.). H.F.E.G. is supported by a Gilead Research Scholar Award in Oncology/Hematology, a ZonMW VENI grant, a grant of the German Research Foundation (CRU344 - GL 1093/1-2), and an Erasmus Medical Center Fellowship.

Authorship

Contribution: U.S.A.S. and S.N.R.F. designed and carried out experiments, analyzed results, and wrote the manuscript; I.A.M.S., S.S., B.B., and H.F.E.G. performed experiments, analyzed and interpreted data, and reviewed the manuscript; A.J.F.D., R.M.H., W.W., T.H., L.S., and K.-V.L. performed bioinformatic analysis and reviewed the manuscript; Y.B.-N. provided compound A51, discussed results, and reviewed the manuscript; R.K.S. obtained funding, designed the study, analyzed data, and wrote the manuscript; and all authors provided critical analysis of the manuscript.

Conflict-of-interest disclosure: Y.B.-N. is a consultant for Edgewood Oncology, a company advancing A51 clinical development for AML/high-risk MDS. The remaining authors declare no competing financial interests.

ORCID profiles: S.S., 0000-0003-1188-2750; W.W., 0000-0002-5083-9838; J.S.-R., 0000-0002-8552-8976; A.J.F.D., 0000-0002-0714-028X; K.-V.L., 0000-0002-1936-298X; Y.B.-N., 0000-0003-1660-715X; H.F.E.G., 0000-0001-6138-8916; R.K.S., 0000-0002-0749-1565.

Correspondence: Rebekka K. Schneider, Cell and Tumor Biology, Rheinisch-Westfälische Technische Hochschule Aachen University Hospital, Pauwelsstrasse 30, 52074 Aachen, Germany; email: reschneider@ukaachen.de.

10. Schneider RK, Ademà V, Heckl D, et al. Role of casein kinase 1A1 in the biology and targeted therapy of del(5q) MDS. *Cancer Cell*. 2014;26(4):509-520.
11. Järås M, Miller PG, Chu LP, et al. Csnk1a1 inhibition has p53-dependent therapeutic efficacy in acute myeloid leukemia. *J Exp Med*. 2014;211(4):605-612.
12. Wang J, Fernald AA, Anastasi J, Le Beau MM, Qian Z. Haploinsufficiency of Apc leads to ineffective hematopoiesis. *Blood*. 2010;115(17):3481-3488.
13. Qian Z, Chen L, Fernald AA, Williams BO, Le Beau MM. A critical role for Apc in hematopoietic stem and progenitor cell survival. *J Exp Med*. 2008;205(9):2163-2175.
14. Bidère N, Ngo VN, Lee J, et al. Casein kinase 1 α governs antigen-receptor-induced NF- κ B activation and human lymphoma cell survival. *Nature*. 2009;458(7234):92-96.
15. Min IM, Pietramaggiore G, Kim FS, Passequé E, Stevenson KE, Wagers AJ. The transcription factor EGR1 controls both the proliferation and localization of hematopoietic stem cells. *Cell Stem Cell*. 2008;2(4):380-391.
16. Joslin JM, Fernald AA, Tennant TR, et al. Haploinsufficiency of EGR1, a candidate gene in the del(5q), leads to the development of myeloid disorders. *Blood*. 2007;110(2):719-726.
17. Stalman USA, Ticconi F, Snoeren IAM, et al. Genetic barcoding systematically compares genes in del(5q) MDS and reveals a central role for CSNK1A1 in clonal expansion. *Blood Adv*. 2022;6(6):1780-1796.
18. Meggendorfer M, Haferlach C, Kern W, Haferlach T. Molecular analysis of myelodysplastic syndrome with isolated deletion of the long arm of chromosome 5 reveals a specific spectrum of molecular mutations with prognostic impact: a study on 123 patients and 27 genes. *Haematologica*. 2017;102(9):1502-1510.
19. Jädersten M, Saft L, Smith A, et al. TP53 mutations in low-risk myelodysplastic syndromes with del(5q) predict disease progression. *J Clin Oncol*. 2011;29(15):1971-1979.
20. Kulasekararaj AG, Smith AE, Mian SA, et al. TP53 mutations in myelodysplastic syndrome are strongly correlated with aberrations of chromosome 5, and correlate with adverse prognosis. *Br J Haematol*. 2013;160(5):660-672.
21. Kastenhuber ER, Lowe SW. Putting p53 in context. *Cell*. 2017;170(6):1062-1078.
22. Olive KP, Tuveson DA, Ruhe ZC, et al. Mutant p53 gain of function in two mouse models of Li-Fraumeni syndrome. *Cell*. 2004;119(6):847-860.
23. Boettcher S, Miller PG, Sharma R, et al. A dominant-negative effect drives selection of missense mutations in myeloid malignancies. *Science*. 2019;365(6453):599-604.
24. Heckl D, Kowalczyk MS, Yudovich D, et al. Generation of mouse models of myeloid malignancy with combinatorial genetic lesions using CRISPR-Cas9 genome editing. *Nat Biotechnol*. 2014;32(9):941-946.
25. Attardi LD, Donehower LA. Probing p53 biological functions through the use of genetically engineered mouse models. *Mutat Res*. 2005;576(1-2):4-21.
26. Iwakuma T, Lozano G. Crippling p53 activities via knock-in mutations in mouse models. *Oncogene*. 2007;26(15):2177-2184.
27. Kelly KR, Nawrocki ST, Espitia CM, et al. Targeting Aurora A kinase activity with the investigational agent alisertib increases the efficacy of cytarabine through a FOXO-dependent mechanism. *Int J Cancer*. 2012;131(11):2693-2703.
28. Triana S, Vonficht D, Jopp-Saile L, et al. Single-cell proteo-genomic reference maps of the hematopoietic system enable the purification and massive profiling of precisely defined cell states. *Nat Immunol*. 2021;22(12):1577-1589.
29. Iacobucci I, Qu C, Varotto E, et al. Modeling and targeting of erythroleukemia by hematopoietic genome editing. *Blood*. 2021;137(12):1628-1640.
30. Weinberg OK, Arber DA. How I diagnose acute leukemia of ambiguous lineage. *Am J Clin Pathol*. 2022;158(1):27-34.
31. Haldar S, Negrini M, Monne M, Sabbioni S, Croce CM. Down-regulation of bcl-2 by p53 in breast cancer cells. *Cancer Res*. 1994;54(8):2095-2097.
32. Liu A, Trairatphisan P, Gjerga E, Didangelos A, Barratt J, Saez-Rodriguez J. From expression footprints to causal pathways: contextualizing large signaling networks with CARNIVAP. *NPJ Syst Biol Appl*. 2019;5:40.
33. Feder K, Edmaier-Schröger K, Rawat VPS, et al. Differences in expression and function of LEF1 isoforms in normal versus leukemic hematopoiesis. *Leukemia*. 2020;34(4):1027-1037.
34. Lodé L, Ménard A, Flet L, et al. Emergence and evolution of mutations are key features of disease progression in myelodysplastic patients with lower-risk del(5q) treated with lenalidomide. *Haematologica*. 2018;103(4):e143-e146.
35. Muto T, Guillamot M, Yeung J, et al. TRAF6 functions as a tumor suppressor in myeloid malignancies by directly targeting MYC oncogenic activity. *Cell Stem Cell*. 2022;29(2):298-314.e9.
36. Qian Z, Fernald AA, Godley LA, Larson RA, Le Beau MM. Expression profiling of CD34+ hematopoietic stem/progenitor cells reveals distinct subtypes of therapy-related acute myeloid leukemia. *Proc Natl Acad Sci U S A*. 2002;99(23):14925-14930.
37. Stoddart A, Nakitandwe J, Chen S-C, Downing JR, Le Beau MM. Haploinsufficient loss of multiple 5q genes may fine-tune Wnt signaling in del(5q) therapy-related myeloid neoplasms. *Blood*. 2015;126(26):2899-2901.
38. Stoddart A, Nakitandwe J, Chen SC, et al. Haploinsufficiency of del(5q) genes, Egr1 and Apc, cooperate with Tp53 loss to induce acute myeloid leukemia in mice. *Blood*. 2015;126(7):1069-1078.
39. Stoddart A, Wang J, Fernald AA, et al. Cytotoxic therapy-induced effects on both hematopoietic and marrow stromal cells promotes therapy-related myeloid neoplasms. *Blood Cancer Discov*. 2020;1(1):32-47.

40. Adema V, Palomo L, Walter W, et al. Pathophysiologic and clinical implications of molecular profiles resultant from deletion 5q. *EBioMedicine*. 2022;80:104059.
41. Walerych D, Lisek K, Del Sal G. Mutant p53: one, no one, and one hundred thousand. *Front Oncol*. 2015;5:289.